ANNUAL REVIEWS

Annual Review of Immunology

Structural Mechanisms of NLRP3 Inflammasome Assembly and Activation

Jianing Fu[1,2] and Hao Wu[1,2]

[1]Department of Biological Chemistry and Molecular Pharmacology, Harvard Medical School, Boston, Massachusetts, USA; email: wu@crystal.harvard.edu

[2]Program in Cellular and Molecular Medicine, Boston Children's Hospital, Boston, Massachusetts, USA

Annu. Rev. Immunol. 2023. 41:301–16

The *Annual Review of Immunology* is online at immunol.annualreviews.org

https://doi.org/10.1146/annurev-immunol-081022-021207

Keywords

NLRP3, ASC, caspase-1, inflammasomes, filaments, structures

Abstract

As an important sensor in the innate immune system, NLRP3 detects exogenous pathogenic invasions and endogenous cellular damage and responds by forming the NLRP3 inflammasome, a supramolecular complex that activates caspase-1. The three major components of the NLRP3 inflammasome are NLRP3, which captures the danger signals and recruits downstream molecules; caspase-1, which elicits maturation of the cytokines IL-1β and IL-18 and processing of gasdermin D to mediate cytokine release and pyroptosis; and ASC (apoptosis-associated speck-like protein containing a caspase recruitment domain), which functions as a bridge connecting NLRP3 and caspase-1. In this article, we review the structural information that has been obtained on the NLRP3 inflammasome and its components or subcomplexes, with special focus on the inactive NLRP3 cage, NEK7 (NIMA-related kinase 7)-licensing of NLRP3 activation, and the PYD-PYD and CARD-CARD homotypic filamentous scaffolds of the inflammasome. We further implicate structure-derived mechanisms for the assembly and activation of the NLRP3 inflammasome.

INTRODUCTION: SELF VERSUS NONSELF AND HARMFUL VERSUS HARMLESS

As the first line of defense, the innate immune system constantly surveys the environment by detecting threatening signs from microbial infections or endogenous cellular damage. It is called innate because the sensing machinery is germline encoded and already exists before pathogen invasion. The mechanism of detection in innate immunity was first proposed as pattern recognition in which molecules conserved in microbes, such as viral nucleic acids, bacterial lipopolysaccharide (LPS), and flagellin, are recognized by pattern recognition receptors (PRRs) to alert the immune system (1). These conserved common microbial molecules are collectively known as pathogen-associated molecular patterns (PAMPs), while molecules released from disrupted or dying cells constitute damage-associated molecular patterns (DAMPs). The concept of pattern recognition preceded the identification of the first PRR, provided a means of distinguishing self versus nonself, and predicted well what the subsequently identified cell surface Toll-like receptors (TLRs) would recognize (2, 3).

However, as more and more intracellular innate immune receptors were identified, it became clear that not all of them directly interact with conserved PAMPs or DAMPs. By contrast, innate immune receptors often sense the danger signals indirectly by detecting cellular changes exerted by PAMPs or DAMPs. Instead of patterns, these receptors recognize perturbations and are thus able to distinguish harmful versus harmless without necessarily discriminating nonself from self, as these perturbations can come from both exogenous and endogenous sources. In most cases, innate immune receptors elicit transcriptional programs such as the expression of cytokines, chemokines, and antimicrobial peptides to exert host defense; sometimes, however, they cause cell death to stop the propagation of pathogens, which is a desperate measure called for by desperate circumstances (3, 4).

In this context, inflammasomes are cytosolic supramolecular complexes that activate caspase-1 or other inflammatory caspases (5–7), and while some inflammasome sensors are PRRs, others are perturbation detectors. One of the most-studied inflammasomes is the NLRP3 inflammasome, which is emerging as a perturbation detector for cellular stress and cell membrane damage. NLRP3 (also known as cryopyrin) belongs to the nucleotide-binding domain (NBD)- and leucine-rich repeat (LRR)-containing protein (NLR) family (5–7). NLRP3 has been found expressed in immune cells of the myeloid lineage like neutrophils, monocytes, and dendritic cells; barrier cells; lymphocytes; and neurons, and it is linked to many human diseases impacting different age groups (8). Genetic aberrations of NLRP3 cause diseases that are collectively called cryopyrin-associated periodic syndrome (CAPS). CAPS is represented by, from less severe to more severe, familial cold autoinflammatory syndrome, Muckle-Wells syndrome, and neonatal-onset multisystem inflammatory disorder, affecting skin, joints, and even the central nervous system (8–11). The NLRP3 inflammasome has also been shown to play an important role in numerous common diseases, from metabolic disorders like type 2 diabetes and obesity to central nervous system conditions like Alzheimer disease and Parkinson disease to various cancers (8–11).

NLRP3 activation requires two steps, a priming step and an activation step. First, NLRP3 expression can be primed by PRRs upon recognition of PAMPs or DAMPs or by cytokines that engage in immune and inflammatory responses. Upon activation of NF-κB or other transcription factors, the expression of NLRP3 and other inflammasome components is transcriptionally upregulated (6, 8, 11, 12). Posttranslational modifications of NLRP3, including ubiquitination, phosphorylation, and sumoylation, also prime NLRP3 for activation while still keeping NLRP3 in an autoinhibited state (8, 11, 12). In the second step, NLRP3 is activated by diverse microbial and sterile stimuli that often converge to K^+ efflux or other ionic changes (5, 11, 13–17).

These stimuli range from bacterial toxins such as nigericin to extracellular ATP to particulates such as uric acid crystals, cholesterol crystals, and amyloids. Importantly, a serine/threonine kinase contributing to mitosis, NEK7 (NIMA-related kinase), has been found to play a critical role in NLRP3 activation through direct binding (18–21). Upon activation, NLRP3 assembles and recruits downstream components to form the inflammasome complex, and the activated inflammatory caspases proteolytically process cytokines to generate the mature forms and induce the highly inflammatory form of cell death known as pyroptosis (5–7, 11).

THE NLRP3 INFLAMMASOME PATHWAY

Formation of the NLRP3 inflammasome, as a signaling cascade, can be separated and defined by three typical components: sensor, adaptor, and effector. These roles are played by NLRP3, ASC (apoptosis-associated speck-like protein containing a caspase recruitment domain), and caspase-1, respectively (5, 6, 11, 22) (**Figure 1*a*,*b***).

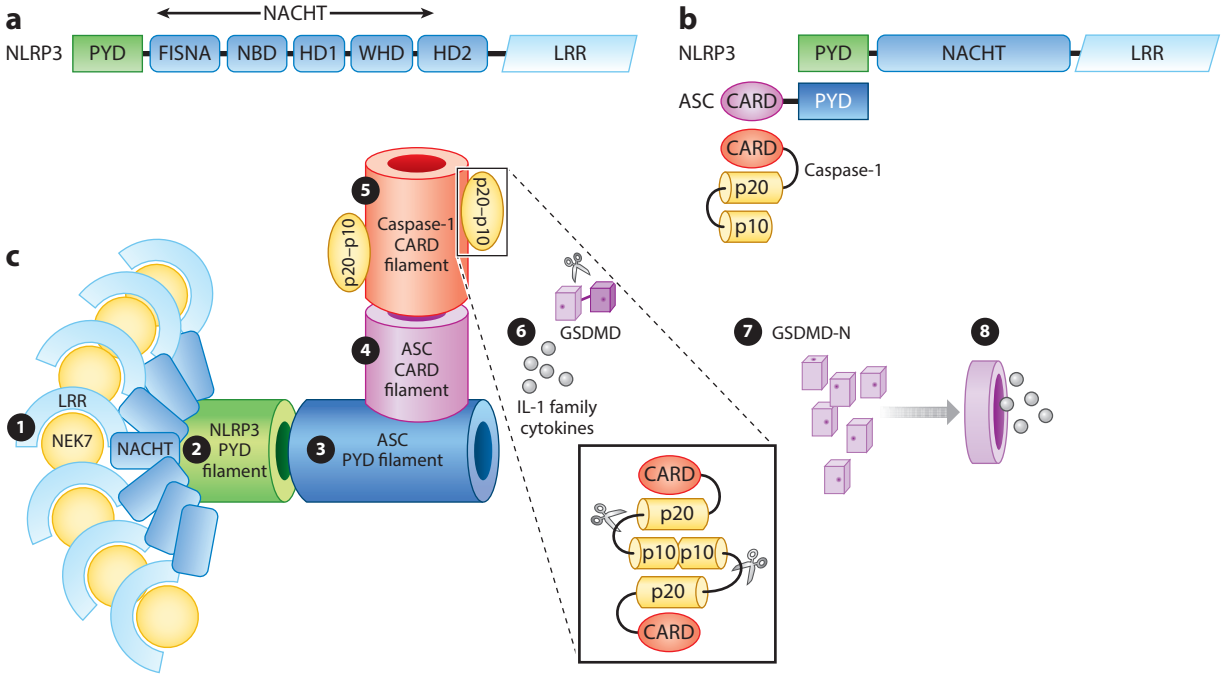

Figure 1

(*a*) NLRP3 domains. (*b*) The sensor-adaptor-effector machinery of the NLRP3 inflammasome, depicting interaction of NLRP3 with ASC through their PYDs, and interaction of ASC with caspase-1 through their CARDs. (*c*) A molecular model of the NLRP3 inflammasome pathway, stepwise from upstream (❶) to downstream (❽). NLRP3 conformational change and the subsequent intracellular trafficking lead to the binding of NLRP3 to NEK7, which induces formation of an NLRP3 inflammasome disk and promotes NLRP3 PYD to form a filament. The NLRP3 PYD filament recruits ASC by nucleating the ASC PYD filament. The CARD of ASC also clusters and forms a filament. The ASC CARD filament recruits caspase-1 by nucleating the caspase-1 CARD filament. The caspase-1 caspase domain (p20/p10) dimerizes and autoprocesses, resulting in its activation. The active caspase-1 then cleaves pro-cytokines in the IL-1 family to generate mature cytokines. Caspase-1 also cleaves GSDMD to generate an active GSDMD N-terminal fragment for membrane pore formation that facilitates cytokine release and pyroptosis. Abbreviations: ASC, apoptosis-associated speck-like protein containing a caspase recruitment domain; CARD, C-terminal caspase recruitment domain; FISNA, fish-specific NACHT-associated domain; GSDMD, gasdermin D; HD1, helical domain 1; LRR, leucine-rich repeat; NBD, nucleotide-binding domain; NEK7, NIMA-related kinase 7; PYD, pyrin domain; WHD, winged helix domain.

The sensor NLRP3 is composed of three parts: an amino (N)-terminal pyrin domain (PYD), a carboxy (C)-terminal LRR, and a central NBD-containing ATPase domain called NACHT (6, 11, 20) (**Figure 1*a***). PYDs usually interact in a homotypic manner to regulate downstream signaling. LRR domains mainly mediate protein-protein interactions, and the LRR of NLRP3 has also been implicated in maintaining NLRP3's stability. NACHT domains, which possess the ability to bind nucleotides and hydrolyze ATP, once triggered, may go through ATP-dependent self-oligomerization resulting in self-PYD interactions that further recruit ASC, the adaptor (6, 11, 20, 23–26) (**Figure 1*b*,*c***).

The adaptor ASC contains an N-terminal PYD and a C-terminal caspase recruitment domain (CARD). It is recruited to the clustered PYDs of the oligomerized NLRP3 molecules by homotypic PYD-PYD interactions, leading to formation of a prion-like ASC filament (26–28). These nucleated filaments gather the C-terminal CARDs of ASC, which act as a platform to recruit caspase-1, the effector (6, 11, 20, 26, 27) (**Figure 1*b*,*c***).

Caspase-1 consists of an N-terminal CARD, a large catalytic subunit called p20, and a C-terminal small catalytic subunit called p10 (29, 30) (**Figure 1*b***). The caspase-1 CARDs interact with the clustered ASC CARDs and undergo similar nucleated filament formation (31, 32). These filaments induce proximity-induced dimerization of the p20 and p10 catalytic subunits of caspase-1 and self-cleavage at the linker between p20 and p10, making caspase-1 fully proteolytically active (29, 33, 34). Although there is no biophysical limit on the range of stoichiometries that these proteins can assume, the relative abundance between ASC and caspase-1 in cells has been estimated as 1:3.5 based on quantitative Western blot (26). Once active, caspase-1 is able to cleave and activate gasdermin D (GSDMD), which is responsible for pyroptosis, and convert the pro-cytokines in the IL-1 family into mature proinflammatory cytokines that are essential for regulating immune responses (6, 11, 26, 29, 35–47) (**Figure 1*c***).

STRUCTURES OF NLRP3 AND MODE OF INHIBITOR BINDING

As a typical NLR, the NACHT domain of NLRP3 is composed of a FISNA (fish-specific NACHT-associated domain), an NBD, a helical domain 1 (HD1), a winged helix domain (WHD), and a helical domain 2 (HD2); the LRR domain comprises multiple LRR repeating units (6, 11, 20, 48–52) (**Figures 1*a*** and **2*a***). The structures of the NACHT and LRR domains of NLRP3 were first revealed from the cryo–electron microscopy (cryo-EM) structure of the NLRP3-NEK7 complex (20) and further supported by subsequent cryo-EM studies on NLRP3 (48–51). Similar to other NLRs like NOD2 and NLRC4 (53–56), the NACHT and LRR domains of NLRP3 show a conserved earring shape (**Figure 2*a***). For NLRP3, the NBD is formed by a central β sheet surrounded by α helices, the HD1, HD2, and WHD are mainly constructed by α helices, and the LRR is structured with 12 repeats (**Figure 2*a***). The FISNA domain, which is partly disordered in inactive NLRP3 and was previously considered part of the NBD, becomes fully ordered in active NLRP3 (57). NBDs, HD1s, and WHDs share comparable architectures among NLRP3, NOD2, and NLRC4. HD2s and LRRs vary in conformation, as HD2s have distinct shapes and orientations and LRRs differ in the number of leucine-rich repeats (12, 10, and 14 repeats in NLRP3, NOD2, and NLRC4, respectively) and curvature (20, 53, 54).

In the inactive state, ADP binds at the nucleotide-binding pocket of NLRP3 within the NACHT domain encircled by WHD, HD1, and NBD (20, 49–51). An inhibitor, MCC950 (also known as CRID3), has been shown to directly inhibit NLRP3 (58). This inhibitor, as well as another inhibitor created using it as the template, has been found binding to the NACHT domain adjacent to ADP (49–51) (**Figure 2*b***). In the active state, ATP is presumably bound to NLRP3, but this conformation has not been captured. The PYD belongs to the death domain (DD) superfamily and exhibits a typical six-helix bundle structure (59, 60) (**Figure 2*c***). The structural details

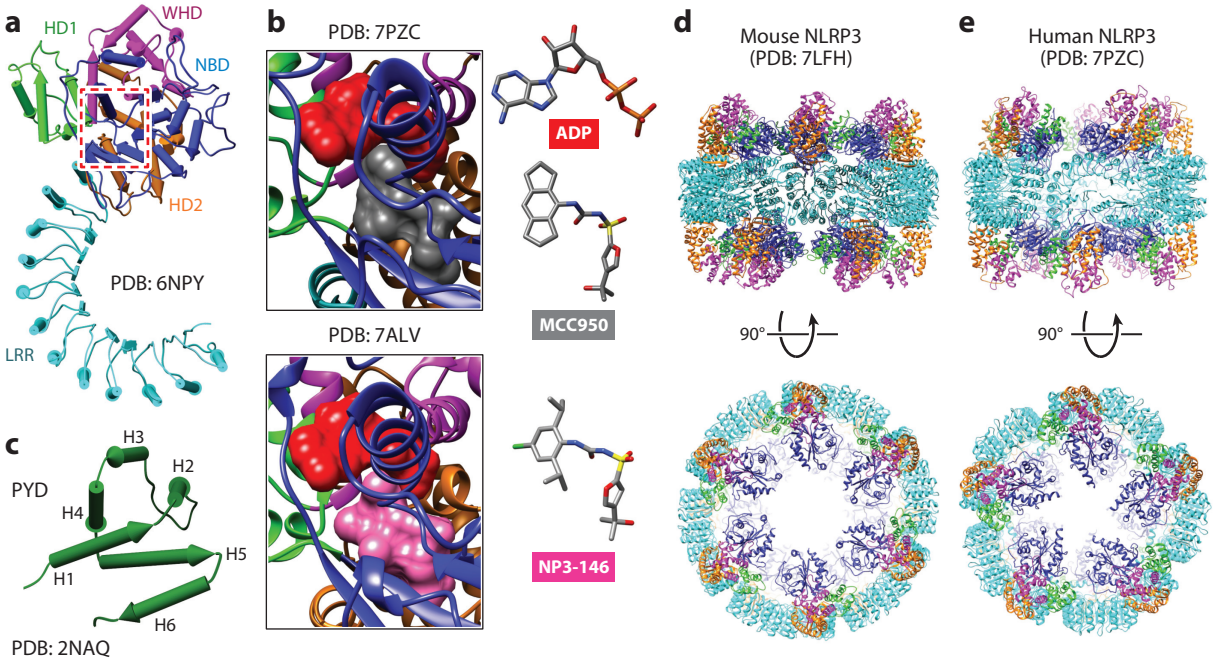

Figure 2

Structures of NLRP3. (*a*) Ribbon diagram of PYD-deleted NLRP3, showing the NACHT and LRR domains. The dashed red rectangle indicates locations for ADP and inhibitors. (*b*) Two examples of the active site of NLRP3 bound to ADP and inhibitors (shown as a surface diagram), illustrating the two adjacent pockets for them. (*c*) Ribbon diagram of the NLRP3 PYD. (*d*) Ribbon diagram of the structure of full-length mouse NLRP3 dodecamer. (*e*) Ribbon diagram of the structure of full-length human NLRP3 decamer. Abbreviations: HD1, helical domain 1; LRR, leucine-rich repeat; NBD, nucleotide-binding domain; PDB, Protein Data Bank; PYD, pyrin domain; WHD, winged helix domain.

of NLRP3 PYD are further described in the section titled PYD-PYD Interactions in the NLRP3 Inflammasome.

NLRP3 OLIGOMERIZATION

Because PYD-deleted NLRP3 used to determine the structure of the NLRP3-NEK7 complex (20) was engineered to be monomeric, to understand NLRP3 in its natural form, the field turned to the full-length NLRP3 protein. Mouse NLRP3s expressed in mammalian cells, without added nucleotides, with the presence of ADP and MCC950, or with dATP (which can be hydrolyzed to dADP), all revealed large oligomeric structures (48) (**Figure 2*d***). NLRP3 particles treated with ADP and MCC950 gave rise to six-, seven-, and eightfold double-ring cage structures of 200 Å to 250 Å, each containing 12, 14, and 16 monomers, respectively, while those treated with dATP were more homogeneously 12-mers and reached the best resolution in the 3D reconstruction (48). The structure of the dodecamer is further supported by a subsequent independent study on full-length mouse NLRP3 (50).

Overall, the two-layer ring-shaped dodecamer, as well as the 14- and 16-mers, looks like a cage or barrel due to the overall circular outline and the hollowness in the center. The dodecamer is formed by 12 monomers following a D6 symmetry, in which the top and bottom surfaces as shown are occupied by 6 NACHT domains that are in inactive conformations and insufficiently close to interact with each other. Importantly, 12 LRR domains encircle the dodecamer, form

its lateral side, and contribute the most to its formation (48, 50). Face-to-face and back-to-back interfaces are formed between neighboring LRR domains from the two rings, in which the LRR domains bind to each other using their concave and convex sides, respectively (48, 50). Residues at these interfaces are critical for the cage formation shown by mutagenesis. The oligomerization of full-length human NLRP3 has also been studied using cryo-EM, and a smaller decameric cage (**Figure 2*e***), similar otherwise to the cage structures from mouse NLRP3, was solved in the presence of ADP and MCC950 (49). Even though the exact oligomeric state varies with species and bound nucleotides, the structural consistency among NLRP3 oligomers is the double-ring organization with each ring possessing 5–8 NLRP3 molecules (48–50).

However, PYDs were not clearly visible in either map of the mouse NLRP3 dodecamer (48, 50). Only weak densities were found in the cage near the center of its top and bottom, presumably representing the PYDs that are flexibly linked in its filamentous form but trapped inside the cavity (48, 50). In support of this assessment, a purified NLRP3 cage sample was not able to nucleate ASC PYDs to form a filament (48). For the human NLRP3 decamer, additional weak densities were also found in the cage, which researchers fitted with a PYD dimer (49). PYDs were shown to play an important role in forming the dodecamer, since PYD deletion compromised cage assembly (48, 50).

Interestingly, purified mouse NLRP3 cage assemblies exhibited membrane binding capability through an affinity to phosphoinositides, and overexpressed mouse NLRP3 was found mostly in the membrane fraction upon cell lysis (48, 50). In addition, endogenous mouse NLRP3 from immortalized bone marrow–derived macrophages was also enriched in the membrane fraction and shown to contain oligomers of similar sizes to purified NLRP3 assemblies, suggesting that the cage structure is a resting state of NLRP3 in cells (48). Importantly, mouse NLRP3 oligomerization on the membrane is a critical step for *trans*-Golgi network dispersion upon NLRP3 stimulation (48), a critical early step in NLRP3 activation (61). These findings also echo previous reports that NLRP3 resides on membranes of various intracellular organelles, including the endoplasmic reticulum, mitochondria, and Golgi apparatus, and is further transported to the microtubule-organizing center where NEK7 is localized (18, 61–70).

While the PYD was shown to be important for cage formation of full-length NLRP3, a recent cryo-EM study of PYD-deleted human NLRP3 with ADP and MCC950 added to stabilize the inactive conformation revealed a spherical hexameric oligomer composed of two layers of trimers (50). This assembly used a similar back-to-back interaction between the LRR domains in the two layers but also contained a head-to-tail interaction of the LRR C terminus of one NLRP3 monomer with the NBD and WHD of the neighboring monomer within the layer (50). It remains to be determined whether the hexamer can also be formed with full-length NLRP3 and what functional role it might play.

STRUCTURAL MECHANISM FOR NEK7-LICENSED NLRP3 ACTIVATION

Human NEK7 is a small serine/threonine kinase that not only plays a prerequisite role in mitosis but is also required for NLRP3 activation (18–20, 71–76). Just like other NEKs, NEK7 contains a smaller 5 β-stranded N lobe and a larger, primarily α-helical C lobe joined by a flexible hinge (71, 77, 78). In the cryo-EM structure of the NLRP3-NEK7 complex, the density for the NEK7 C lobe was found, whereas the density for NEK7 N lobe was not visible. When the full-length NEK7 structure is overlaid on the NLRP3-NEK7 map, with the C lobe nicely fitted, the N lobe does not sterically interfere with the complex, indicating that the NEK7 N lobe presumably does not participate in the NLRP3 interaction (20).

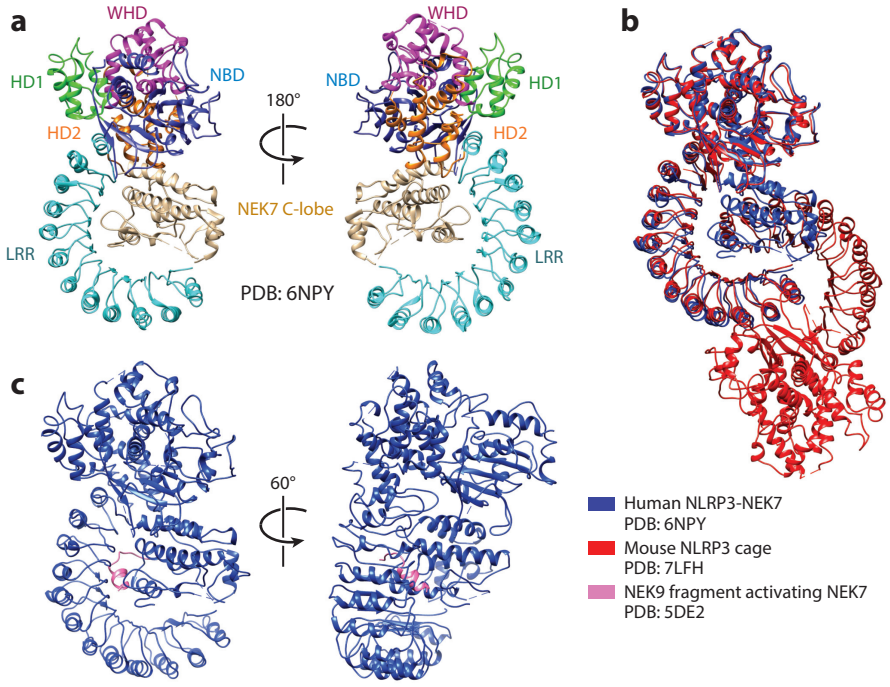

Figure 3

The NLRP3-NEK7 complex. (*a*) Ribbon diagram of the structure of NLRP3 in complex with the NEK7 C-lobe viewed from two directions. The structure is colored by domain. (*b*) Superposition of the NLRP3-NEK7 complex (*blue*) with two monomers in an NLRP3 cage (*red*), showing that these two interactions compete with each other. (*c*) The position of NEK9 (*pink*) while interacting with NEK7 shows its competition with NLRP3 for NEK7, indicating that it is unlikely that NEK7-licensed NLRP3 activation and NEK9-induced NEK7 activation in mitosis will occur simultaneously. Abbreviations: HD1, helical domain 1; LRR, leucine-rich repeat; NBD, nucleotide-binding domain; NEK7, NIMA-related kinase 7; PDB, Protein Data Bank; WHD, winged helix domain.

The density of the NEK7 C lobe is encircled by the NLRP3 LRR domain, with its first half interacting with the LRR and its second half interacting with the NBD and HD2 in NACHT (20) (**Figure 3*a***). The isoelectric points of NLRP3 and the NEK7 C lobe are 6.2 and 9.0, respectively, suggesting that the interactions between the two are largely based on electrostatic complementarity. Importantly, according to mutagenesis studies, only the LRR and HD2, but not the NBD, have crucial contributions in the NLRP3-NEK7 binding interface (20). Nevertheless, the significance of the NBD in NLRP3 activation should not be ignored, given that the NBD contains more disease-related mutations compared to other subdomains in NACHT; these mutated residues, involved in ATP binding or catalysis or simply buried inside their own domains, may destabilize the inactive conformation of NLRP3 to trigger downstream immune activities (20, 79).

While NLRP3 can both self-associate and interact with NEK7, since the concave side of the NLRP3 LRR domain acts as a binding site not only for NEK7 but also for NLRP3 self-assembly in the cage structures, NEK7 interaction is mutually exclusive with cage formation, due to steric clash (48, 50) (**Figure 3*b***). Indeed, when given access to NEK7, purified NLRP3 cages decreased in amount and smaller NLRP3 species appeared, suggesting that NEK7 competes with the NLRP3–NLRP3 binding sites to disrupt the double-ring cages, which should occur when NLRP3 is transported to the microtubule-organizing center and colocalized with NEK7 (48).

The involvement of NEK7 in NLRP3 inflammasome biology has additional implications. The first half of the NEK7 C lobe not only participates in binding to NLRP3 but also is involved in the interaction with NEK9 during mitosis (80). Since the binding site on NEK7 is partially shared between NLRP3 and NEK9, it is likely that when the amount of NEK7 is restricted, NLRP3 activation and mitosis negatively regulate each other (20, 21, 80) (**Figure 3*c***).

THE ACTIVE NLRP3 INFLAMMASOME DISK

Even though much information has been gained from inactive-state NLRP3 structures, the active-state conformation and assembly of NLRP3 were only predicted based on the known active NLRC4 structure (20, 55, 56), until now. The new active NLRP3 inflammasome disk (**Figure 4*a*,*b***) finally revealed its conformational change, nucleotide exchange, and mode of assembly (57).

Xiao et al. (57) reconstituted the active NLRP3 inflammasome with three major components, NLRP3, NEK7, and ASC, in which NEK7 binds to the LRR domain of NLRP3 and ASC stabilizes the inflammasome assembly by forming a PYD-PYD filament with NLRP3. The filament is observed as long threadlike tails under negative staining electron microscopy, and the cryo-EM structure of the filament is similar to those in previously published studies (26, 49, 81), which are covered in the next section, titled PYD-PYD Interactions in the NLRP3 Inflammasome. Importantly, this active conformation is locked by an ATP analog, adenosine 5′-*O*-(3-thio) triphosphate (ATPγS), which mimics the ATP and binds to NACHT of NLRP3 (57) (**Figure 4*d*,*e***).

Cryo-EM reconstruction resulted in two flower-shaped disks that comprise 10 subunits and 11 subunits, respectively, of the NLRP3-NEK7-ASC complex, and some partial disks that comprise mainly 5 subunits. The PYD filaments formed between NLRP3 and ASC are observed only in full disks, not partial disks, suggesting only full disks are able to recruit ASC effectively. The 10-subunit disk, with a diameter of about 320 Å, has been used for further analysis (**Figure 4*a*,*b***). The NLRP3 NACHT domain interacts in the center of the disk, with mainly NBD, WHD, and HD2 on one side and FISNA and HD1 on the other side. NEK7-bound NLRP3 LRR is located away from the center (**Figure 4*a*,*b***), indicating that neither NLRP3 LRR nor NEK7 directly participates in the disk assembly. Indeed, instead of contributing to interactions among NLRP3 protomers, NEK7 may play a role in breaking the inactive NLRP3 cage (57).

Dramatic conformational changes are found when NLRP3 turns from inactive to active. The WHD-HD2-LRR region undergoes a rigid body rotation of about 85.4° while superimposing the FISNA-NBD-HD1 regions of the active and inactive NLRP3 (**Figure 4*c***). In particular, the FISNA region has very important roles in disk assembly. FISNA not only participates in ATPγS binding (**Figure 4*d*,*e***) but also engages in the interactions between NLRP3 molecules in the disk (**Figure 4*a*,*b***). Specifically, as a region partially disordered in inactive NLRP3, FISNA becomes fully ordered in active NLRP3. The ordered loop 1 and loop 2 of FISNA, together with HD1 and a β-hairpin loop of WHD, bridge and stabilize two neighboring NLRP3s in the disk (57).

Based on the active NLRP3 disk and the inactive NLRP3 structures, including the oligomeric cages (48–50) and NLRP3 in complex with NEK7 (20) discussed in the previous two sections, Xiao et al. (57) proposed that the NLRP3 inflammasome pathway might contain the following steps: priming and upregulation of NLRP3 expression, NLRP3 oligomeric cage formation in the *trans*-Golgi network, *trans*-Golgi network dispersion and vesicle trafficking to the microtubule-organizing center, NLRP3 cage opening by NEK7 binding, and active NLRP3 disk assembly (**Figure 4*f***). The last two steps indicate a possibility that the full disk is formed by two half-rings of the NLRP3 cage that rearrange after cage dissociation (57). The subsequent steps include the nucleation and filament formation of NLRP3 PYD in the center of the disk, which are followed by ASC recruitment and formation of the hybrid PYD-PYD filament between NLRP3 and ASC.

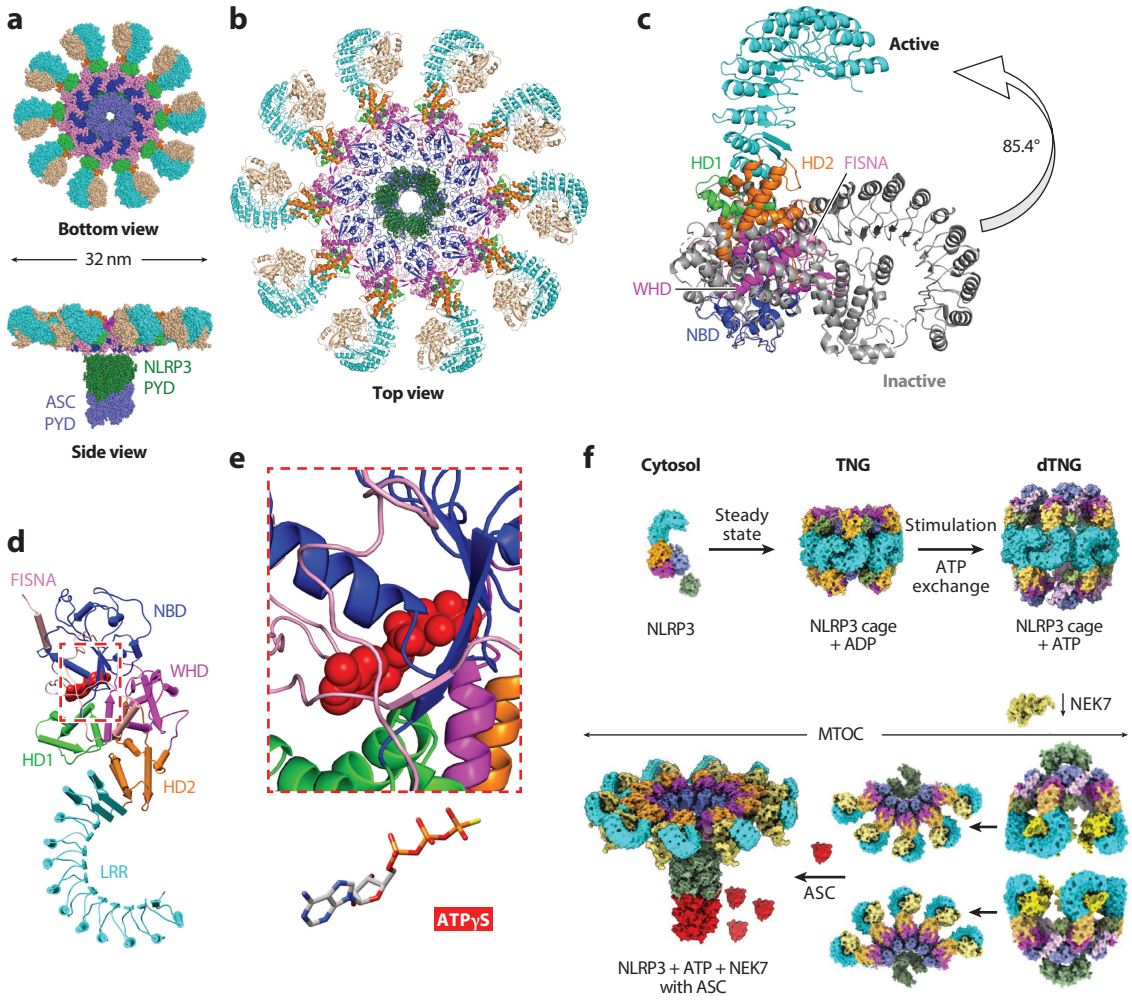

Figure 4

Details on the active NLRP3 inflammasome disk. NLRP3 molecules are colored based on domains. (*a*) Surface view of the active NLRP3 inflammasome disk viewed from bottom and side, with the nucleated PYD-PYD filament formed by NLRP3 PYD (*dark green*) and ASC PYD (*light purple*) in the center of the disk (PDB: 8EJ4). (*b*) Ribbon diagram of the active NLRP3 inflammasome disk viewed from the top (PDB: 8EJ4). (*c*) Ribbon diagram showing the rigid body rotation of NLRP3 turning from inactive (*gray*) (PDB: 6NPY) to active (PDB: 8EJ4). (*d*) Ribbon diagram of NLRP3 showing only NACHT and LRR domains with the bounded ATP analog, ATPγS (shown as surface view) (PDB: 8EJ4). (*e*) A zoomed-in view of the active site of NLRP3 bound to ATPγS (shown as surface view) (PDB: 8EJ4). (*f*) A proposed NLRP3 activation model based on structures. Abbreviations: ASC, apoptosis-associated speck-like protein containing a caspase recruitment domain; ATPγS, adenosine 5′-*O*-(3-thio) triphosphate; FISNA, fish-specific NACHT-associated domain; HD1, helical domain 1; LRR, leucine-rich repeat; MTOC, microtubule-organizing center; NBD, nucleotide-binding domain; NEK7, NIMA-related kinase 7; PDB, Protein Data Bank; PYD, pyrin domain; WHD, winged helix domain. Structural illustrations in panels *a*–*e* are based on data from Reference 57. Panel *f* adapted from Reference 57.

PYD-PYD INTERACTIONS IN THE NLRP3 INFLAMMASOME

The adaptor protein ASC has an N-terminal PYD and a C-terminal CARD and bridges NLRP3 to caspase-1. Upon NLRP3 stimulation, full-length endogenous ASC molecules interact with NLRP3 through PYD-PYD interactions (6, 11, 26–28), and with caspase-1 through

CARD-CARD interactions (6, 11, 31, 32), to form speck-like aggregates (82, 83). The ASC specks presumably contain cross-linked PYD and CARD filaments, as ASC-PYD-only and ASC-CARD-only fragments form long filaments in cells (84), which suggests the polymerization property of the ASC protein (26, 83, 85). Specifically, PYD-PYD and CARD-CARD interactions are two types of homotypic interactions undergoing nucleation-polymerization that are involved in the signaling and formation of the NLRP3 inflammasome (26).

PYDs constitute a family of domains in the DD superfamily whose members share a six-helix bundle structure and form homotypic interactions for inflammatory signaling (59, 60, 85, 86). The PYD structures of NLRP3 and ASC are highly similar, each composed of six antiparallel helices (α1–α6), among which α1, α2, and α4–α6 are closely packed together to form a central hydrophobic core, whereas α3 is often shorter and more external (26, 28, 60, 87) (**Figure 2*c***). Even though NLRP3 and ASC PYDs share overall structural similarities with other PYDs, such as those of NLRP1, NLRP7, and NLRP10, the α2-α3 loop, which undergoes conformational change in filament formation (see below), is the most divergent.

The first PYD filament structure was revealed from the cryo-EM structure of the ASC PYD filament (26), and the recently reported structure of the NLRP3 filament has a similar structural architecture (81) (**Figure 5*a*,*b***). The ASC PYD filament structure shows a three-start helical assembly following a C3 point group symmetry with the subunits packed to each other spirally as helical strands that contain a right-handed rotation of ∼53° and an axial rise of ∼14 Å per subunit. The overall shape of the filament is cylindrical, with an outer diameter of ∼90 Å and an inner diameter of ∼20 Å that defines the central hollow channel (26). Filament formation is contributed by strong charge complementarity, suggested by the highly positive and highly negative opposing sides at the cross section of the filament (26). Even though the NLRP3 PYD has limited sequence identity to the ASC PYD, its helical symmetry in rotation and axial rise per subunit are almost the same, as well as the charge complementarity in the assembly of the filament (81).

PYD filaments are polar filaments in that they polymerize unidirectionally due to the requirement for conformational change during filament formation. For the ASC PYD, conformational differences between the NMR (nuclear magnetic resonance) structure of the ASC PYD in solution (28) and the cryo-EM structure of the ASC PYD in the filament have been observed, especially at the α2-α3 loop that participates in the typical asymmetric interactions in the filament, types I, II, and III (26, 85, 86) (**Figure 5*c***). Type I interactions are formed by α1 and α4 residues of one subunit and α2 and α3 residues on the neighboring intrastrand subunit; type II interactions are formed by α4-α5 corner residues of one subunit and α5-α6 corner residues of the neighboring interstrand subunit; and type III interactions are formed by α2-α3 corner residues of one subunit and α1-α2 corner residues of the neighboring interstrand subunit (26, 85, 86).

It has been modeled that oligomerized NLRP3 PYDs nucleate ASC PYD filament formation, and experimentally, activated NLRP3 induces ASC to become filamentous (26, 81) (**Figure 5*d***). The similarities in architecture and charge distribution of the filaments explain how ASC PYD subunits could be recruited to an NLRP3 PYD filament and elongate to form the connected ASC PYD filament. In the NLRP3 inflammasome, it is likely that the nucleated ASC PYD filament gathers ASC CARDs to provide a platform for recruiting the effector caspase-1 through CARD-CARD interactions (26).

CARD-CARD INTERACTIONS AND CASPASE ACTIVATION

Like PYDs, CARDs also belong to the DD superfamily, and the ASC CARD and caspase-1 CARD both exhibit a six-helix bundle structure, as revealed from crystal and NMR structures of the individual subunits and cryo-EM structures of the corresponding filaments (28, 31, 32, 88–91).

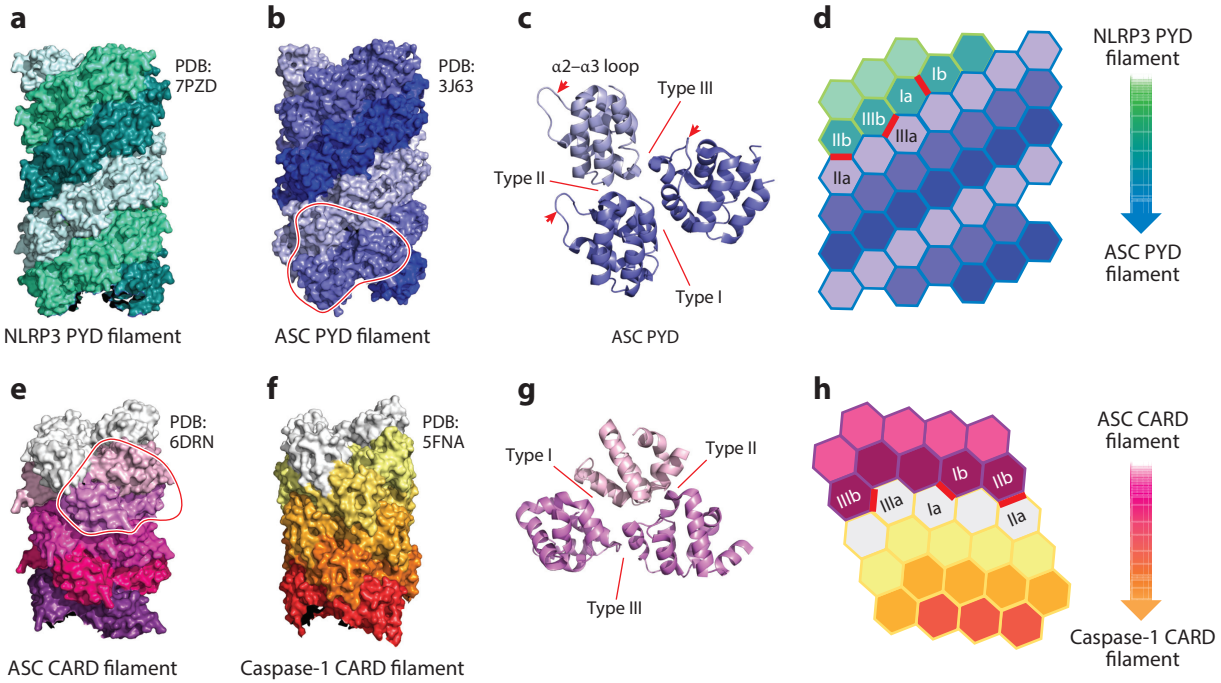

Figure 5

PYD-PYD and CARD-CARD interactions. (*a*) Surface diagram of the NLRP3 PYD filament, colored in three shades of green, for each of the three helical strands. (*b*) Surface diagram of the ASC PYD filament, colored in three shades of blue, for each of the three helical strands. The red outline encloses three ASC PYD subunits. (*c*) Enlarged view of the enclosed ASC PYD subunits in panel *b*, showing locations of type I, II, and III interactions (*red leader lines*) and the highly variable α2-α3 loop (*red arrowheads*). (*d*) Schematic organization of the NLRP3 PYD–ASC PYD helical filament in which NLRP3 (*green*) nucleates PYD to form an ASC filament (*blue*). The vertical arrow indicates the direction of filament polymerization, and the red lines indicate the locations of type I, II, and III interactions. (*e*) Surface diagram of the ASC CARD filament, colored in different shades of pink along the helix. The red outline encloses three ASC CARD subunits. (*f*) Surface diagram of the caspase-1 CARD filament, colored in different shades of orange along the helix. (*g*) Enlarged view of the enclosed ASC CARD subunits in panel *e*, showing locations of type I, II, and III interactions (*red leader lines*). (*h*) Schematic organization of the ASC CARD–caspase-1 CARD helical filament in which ASC (*pink*) nucleates caspase-1 to form a filament (*orange*). The vertical arrow indicates the direction of filament polymerization, and the red lines indicate the locations of type I, II, and III interactions. Abbreviations: ASC, apoptosis-associated speck-like protein containing a caspase recruitment domain; CARD, C-terminal caspase recruitment domain; PDB, Protein Data Bank; PYD, pyrin domain.

The cryo-EM structures of the caspase-1 CARD filament (31) and the ASC CARD filament (31, 32, 88, 89, 91) display an overall cylindrical shape with a central hole that is similar to that of the ASC PYD filament (26), with an outer diameter of ∼80 Å and an inner diameter of less than 10 Å (**Figure 5*e*,*f***). However, unlike the PYD filaments described above, the caspase-1 and ASC CARD filaments have a left-handed, one-start helical symmetry with an approximately −100° rotation and 5 Å in rise per subunit. As learned from PYD filament structures, three interaction types are also found. However, the type III interface is formed within the helical strand, whereas type I and II interfaces are formed between subunits on different strands and contribute more to filament formation; the type I interface is the most extensive type among the three (**Figure 5*g***). One of the two sides of a cross section of the caspase-1 CARD and the ASC CARD filaments is highly negative and the other highly positive, suggesting that charge complementarity is essential for the formation of these filaments (31, 32).

It is further suggested that the caspase-1 CARD filaments are nucleated and assembled unidirectionally and hierarchically by the upper-stream ASC CARD filaments (**Figure 5*b***), mediating the heterooligomeric CARD-CARD interactions through charge and shape complementarity (31, 32, 91). This direct recruitment of the caspase-1 CARD by the ASC CARD was further demonstrated in an engineered fusion construct of the ASC CARD and caspase-1 CARD, which revealed an octameric CARD filament with four ASC CARD molecules and four caspase-1 CARD molecules (91). Once recruited through CARD-CARD interactions, caspase-1 catalytic domains dimerize to become activated, as previously reported, and then proteolytically mediate GSDMD activation and cytokine maturation (29, 30, 33, 34, 92).

The different autoprocessed forms of caspase-1 exhibit differential activities toward cell death and cytokine maturation (**Figure 1*c***). The full-length caspase-1 dimers, also called p46, efficiently process GSDMD, leading to the formation of large transmembrane β-barrel pores by the GSDMD N-terminal fragment to drive pyroptosis (6, 11, 29, 33, 34, 39–45, 47). When the linker between p20 and p10 within the catalytic domain is autoprocessed, the resulting p33/p10 caspase-1 contains full catalytic functions to process more substrates other than GSDMD, including many proinflammatory cytokines like IL-1β and IL-18, as earlier studies revealed (6, 29, 30, 35–38, 46). The matured cytokines leave the cell through GSDMD pores (40, 42, 44, 45, 93, 94). Upon the subsequent autocleavage at the CARD domain linker, the resulting p20/p10 caspase-1 is released from the inflammasome complex, becomes unstable in cells, and loses protease activity (29).

CONCLUSIONS: DIVERSE MECHANISMS FOR DIVERSE NLR PROTEINS

As a perturbation sensor for cell membrane damage, the NLRP3 inflammasome has attracted much attention in recent years for its broad biology in signaling, inflammation, and cell death; its association with congenital and acquired human diseases; and its potential as a therapeutic target. Structural discoveries on the NLRP3 inflammasome have provided critical insights on how proteins in the supramolecular complex cooperate with each other to assemble and activate caspase-1. Together with light microscopy and other cell biological studies, these structural insights have implicated a complex NLRP3 activation mechanism that requires extensive intracellular trafficking, in addition to the protein-protein interactions that dictate the assembly. NLRP3 belongs to the NLR family of proteins, many of which assemble inflammasomes.

The studies on NLRP3 reviewed here contrast mechanisms revealed by other NLR inflammasomes. The NLRP1 inflammasome, for example, senses unusual intracellular protease or ubiquitin ligase activity from pathogens or intrinsic stress and becomes activated through regulated proteolysis of the N-terminal region of NLRP1 to release the active C-terminal region for filament formation, ASC recruitment, and caspase-1 activation (88, 91, 94, 95). Other NLR inflammasomes, the NLRP6 inflammasomes involved in host defense in the gut and the liver, were shown to interact directly with dsRNA (a PAMP) to form liquid-liquid phase separation, which in turn raised the local concentration of NLRP6 to recruit ASC and caspase-1 (96). Thus, while these NLR inflammasomes converge to the same outcome of caspase-1 activation, they achieve the outcome using diverse mechanisms, illustrating how structures serve their functions. Future studies may reveal further unexpected structure and biology for the family of NLR inflammasomes.

DISCLOSURE STATEMENT

H.W. is a cofounder of Ventus Therapeutics. The authors are not aware of any other affiliations, memberships, funding, or financial holdings that might be perceived as affecting the objectivity of this review.

LITERATURE CITED

1. Janeway CA Jr. 1989. Approaching the asymptote? Evolution and revolution in immunology. *Cold Spring Harb. Symp. Quant. Biol.* 54(Part 1):1–13
2. Kawai T, Akira S. 2010. The role of pattern-recognition receptors in innate immunity: update on Toll-like receptors. *Nat. Immunol.* 11:373–84
3. Li D, Wu M. 2021. Pattern recognition receptors in health and diseases. *Signal Transduct. Target Ther.* 6:291
4. Vora SM, Lieberman J, Wu H. 2021. Inflammasome activation at the crux of severe COVID-19. *Nat. Rev. Immunol.* 21:694–703
5. Gaidt MM, Hornung V. 2018. The NLRP3 inflammasome renders cell death pro-inflammatory. *J. Mol. Biol.* 430:133–41
6. Schroder K, Tschopp J. 2010. The inflammasomes. *Cell* 140:821–32
7. Broz P, Dixit VM. 2016. Inflammasomes: mechanism of assembly, regulation and signalling. *Nat. Rev. Immunol.* 16:407–20
8. Sharma M, de Alba E. 2021. Structure, activation and regulation of NLRP3 and AIM2 inflammasomes. *Int. J. Mol. Sci.* 22:872
9. Wang Z, Zhang S, Xiao Y, Zhang W, Wu S, et al. 2020. NLRP3 inflammasome and inflammatory diseases. *Oxid. Med. Cell Longev.* 2020:4063562
10. Zahid A, Li B, Kombe AJK, Jin T, Tao J. 2019. Pharmacological inhibitors of the NLRP3 inflammasome. *Front. Immunol.* 10:2538
11. Swanson KV, Deng M, Ting JP. 2019. The NLRP3 inflammasome: molecular activation and regulation to therapeutics. *Nat. Rev. Immunol.* 19:477–89
12. Gritsenko A, Green JP, Brough D, Lopez-Castejon G. 2020. Mechanisms of NLRP3 priming in inflammaging and age related diseases. *Cytokine Growth Factor Rev.* 55:15–25
13. Munoz-Planillo R, Kuffa P, Martinez-Colon G, Smith BL, Rajendiran TM, Nunez G. 2013. K^+ efflux is the common trigger of NLRP3 inflammasome activation by bacterial toxins and particulate matter. *Immunity* 38:1142–53
14. Murakami T, Ockinger J, Yu J, Byles V, McColl A, et al. 2012. Critical role for calcium mobilization in activation of the NLRP3 inflammasome. *PNAS* 109:11282–87
15. Green JP, Yu S, Martin-Sanchez F, Pelegrin P, Lopez-Castejon G, et al. 2018. Chloride regulates dynamic NLRP3-dependent ASC oligomerization and inflammasome priming. *PNAS* 115: E9371–80
16. Campden RI, Zhang Y. 2019. The role of lysosomal cysteine cathepsins in NLRP3 inflammasome activation. *Arch. Biochem. Biophys.* 670:32–42
17. Zhong Z, Liang S, Sanchez-Lopez E, He F, Shalapour S, et al. 2018. New mitochondrial DNA synthesis enables NLRP3 inflammasome activation. *Nature* 560:198–203
18. Fry AM, O'Regan L, Sabir SR, Bayliss R. 2012. Cell cycle regulation by the NEK family of protein kinases. *J. Cell Sci.* 125:4423–33
19. He Y, Zeng MY, Yang D, Motro B, Nunez G. 2016. NEK7 is an essential mediator of NLRP3 activation downstream of potassium efflux. *Nature* 530:354–57
20. Sharif H, Wang L, Wang WL, Magupalli VG, Andreeva L, et al. 2019. Structural mechanism for NEK7-licensed activation of NLRP3 inflammasome. *Nature* 570:338–43
21. Shi H, Wang Y, Li X, Zhan X, Tang M, et al. 2016. NLRP3 activation and mitosis are mutually exclusive events coordinated by NEK7, a new inflammasome component. *Nat. Immunol.* 17:250–58
22. Wang L, Sharif H, Vora SM, Zheng Y, Wu H. 2021. Structures and functions of the inflammasome engine. *J. Allergy Clin. Immunol.* 147:2021–29
23. Moasses Ghafary S, Soriano-Teruel PM, Lotfollahzadeh S, Sancho M, Serrano-Candelas E, et al. 2022. Identification of $NLRP3^{PYD}$ homo-oligomerization inhibitors with anti-inflammatory activity. *Int. J. Mol. Sci.* 23:1651
24. Jin C, Flavell RA. 2010. Molecular mechanism of NLRP3 inflammasome activation. *J. Clin. Immunol.* 30:628–31
25. Niu T, De Rosny C, Chautard S, Rey A, Patoli D, et al. 2021. NLRP3 phosphorylation in its LRR domain critically regulates inflammasome assembly. *Nat. Commun.* 12:5862

26. Lu A, Magupalli VG, Ruan J, Yin Q, Atianand MK, et al. 2014. Unified polymerization mechanism for the assembly of ASC-dependent inflammasomes. *Cell* 156:1193–206
27. Cai X, Chen J, Xu H, Liu S, Jiang QX, et al. 2014. Prion-like polymerization underlies signal transduction in antiviral immune defense and inflammasome activation. *Cell* 156:1207–22
28. de Alba E. 2009. Structure and interdomain dynamics of apoptosis-associated speck-like protein containing a CARD (ASC). *J. Biol. Chem.* 284:32932–41
29. Boucher D, Monteleone M, Coll RC, Chen KW, Ross CM, et al. 2018. Caspase-1 self-cleavage is an intrinsic mechanism to terminate inflammasome activity. *J. Exp. Med.* 215:827–40
30. Thornberry NA, Bull HG, Calaycay JR, Chapman KT, Howard AD, et al. 1992. A novel heterodimeric cysteine protease is required for interleukin-1β processing in monocytes. *Nature* 356:768–74
31. Lu A, Li Y, Schmidt FI, Yin Q, Chen S, et al. 2016. Molecular basis of caspase-1 polymerization and its inhibition by a new capping mechanism. *Nat. Struct. Mol. Biol.* 23:416–25
32. Li Y, Fu TM, Lu A, Witt K, Ruan J, et al. 2018. Cryo-EM structures of ASC and NLRC4 CARD filaments reveal a unified mechanism of nucleation and activation of caspase-1. *PNAS* 115:10845–52
33. Broz P, von Moltke J, Jones JW, Vance RE, Monack DM. 2010. Differential requirement for Caspase-1 autoproteolysis in pathogen-induced cell death and cytokine processing. *Cell Host Microbe* 8:471–83
34. Ross C, Chan AH, Von Pein J, Boucher D, Schroder K. 2018. Dimerization and auto-processing induce caspase-11 protease activation within the non-canonical inflammasome. *Life Sci Alliance* 1:e201800237
35. Raupach B, Peuschel SK, Monack DM, Zychlinsky A. 2006. Caspase-1-mediated activation of interleukin-1β (IL-1β) and IL-18 contributes to innate immune defenses against *Salmonella enterica* serovar Typhimurium infection. *Infect. Immun.* 74:4922–26
36. Dinarello CA, Novick D, Kim S, Kaplanski G. 2013. Interleukin-18 and IL-18 binding protein. *Front. Immunol.* 4:289
37. Lalor SJ, Dungan LS, Sutton CE, Basdeo SA, Fletcher JM, Mills KH. 2011. Caspase-1-processed cytokines IL-1β and IL-18 promote IL-17 production by γδ and CD4 T cells that mediate autoimmunity. *J. Immunol.* 186:5738–48
38. Sansonetti PJ, Phalipon A, Arondel J, Thirumalai K, Banerjee S, et al. 2000. Caspase-1 activation of IL-1β and IL-18 are essential for *Shigella flexneri*-induced inflammation. *Immunity* 12:581–90
39. Ding J, Wang K, Liu W, She Y, Sun Q, et al. 2016. Pore-forming activity and structural autoinhibition of the gasdermin family. *Nature* 535:111–16
40. Liu X, Zhang Z, Ruan J, Pan Y, Magupalli VG, et al. 2016. Inflammasome-activated gasdermin D causes pyroptosis by forming membrane pores. *Nature* 535:153–58
41. Liu Z, Wang C, Yang J, Chen Y, Zhou B, et al. 2020. Caspase-1 engages full-length gasdermin D through two distinct interfaces that mediate caspase recruitment and substrate cleavage. *Immunity* 53:106–14.e5
42. Xia S, Zhang Z, Magupalli VG, Pablo JL, Dong Y, et al. 2021. Gasdermin D pore structure reveals preferential release of mature interleukin-1. *Nature* 593:607–11
43. Yang J, Liu Z, Wang C, Yang R, Rathkey JK, et al. 2018. Mechanism of gasdermin D recognition by inflammatory caspases and their inhibition by a gasdermin D-derived peptide inhibitor. *PNAS* 115:6792–97
44. Sborgi L, Ruhl S, Mulvihill E, Pipercevic J, Heilig R, et al. 2016. GSDMD membrane pore formation constitutes the mechanism of pyroptotic cell death. *EMBO J.* 35:1766–78
45. Shi J, Zhao Y, Wang K, Shi X, Wang Y, et al. 2015. Cleavage of GSDMD by inflammatory caspases determines pyroptotic cell death. *Nature* 526:660–65
46. Martinon F, Burns K, Tschopp J. 2002. The inflammasome: a molecular platform triggering activation of inflammatory caspases and processing of proIL-β. *Mol. Cell* 10:417–26
47. Kayagaki N, Stowe IB, Lee BL, O'Rourke K, Anderson K, et al. 2015. Caspase-11 cleaves gasdermin D for non-canonical inflammasome signalling. *Nature* 526:666–71
48. Andreeva L, David L, Rawson S, Shen C, Pasricha T, et al. 2021. NLRP3 cages revealed by full-length mouse NLRP3 structure control pathway activation. *Cell* 184:6299–312.e22
49. Hochheiser IV, Pilsl M, Hagelueken G, Moecking J, Marleaux M, et al. 2022. Structure of the NLRP3 decamer bound to the cytokine release inhibitor CRID3. *Nature* 604:184–89
50. Ohto U, Kamitsukasa Y, Ishida H, Zhang Z, Murakami K, et al. 2022. Structural basis for the oligomerization-mediated regulation of NLRP3 inflammasome activation. *PNAS* 119:e2121353119

51. Dekker C, Mattes H, Wright M, Boettcher A, Hinniger A, et al. 2021. Crystal structure of NLRP3 NACHT domain with an inhibitor defines mechanism of inflammasome inhibition. *J. Mol. Biol.* 433:167309
52. Tapia-Abellán A, Angosto-Bazarra D, Alarcón-Vila C, Baños MC, Hafner-Bratkovič I, et al. 2021. Sensing low intracellular potassium by NLRP3 results in a stable open structure that promotes inflammasome activation. *Sci. Adv.* 7(38):eabf4468
53. Hu Z, Yan C, Liu P, Huang Z, Ma R, et al. 2013. Crystal structure of NLRC4 reveals its autoinhibition mechanism. *Science* 341:172–75
54. Maekawa S, Ohto U, Shibata T, Miyake K, Shimizu T. 2016. Crystal structure of NOD2 and its implications in human disease. *Nat. Commun.* 7:11813
55. Zhang L, Chen S, Ruan J, Wu J, Tong AB, et al. 2015. Cryo-EM structure of the activated NAIP2-NLRC4 inflammasome reveals nucleated polymerization. *Science* 350:404–9
56. Hu Z, Zhou Q, Zhang C, Fan S, Cheng W, et al. 2015. Structural and biochemical basis for induced self-propagation of NLRC4. *Science* 350:399–404
57. Xiao L, Magupalli VG, Wu H. 2022. Cryo-EM structures of the active NLRP3 inflammasome disk. *Nature*. In press. **https://doi.org/10.1038/s41586-022-05570-8**
58. Coll RC, Robertson AA, Chae JJ, Higgins SC, Munoz-Planillo R, et al. 2015. A small-molecule inhibitor of the NLRP3 inflammasome for the treatment of inflammatory diseases. *Nat. Med.* 21:248–55
59. Park HH, Lo YC, Lin SC, Wang L, Yang JK, Wu H. 2007. The death domain superfamily in intracellular signaling of apoptosis and inflammation. *Annu. Rev. Immunol.* 25:561–86
60. Bae JY, Park HH. 2011. Crystal structure of NALP3 protein pyrin domain (PYD) and its implications in inflammasome assembly. *J. Biol. Chem.* 286:39528–36
61. Chen J, Chen ZJ. 2018. PtdIns4P on dispersed *trans*-Golgi network mediates NLRP3 inflammasome activation. *Nature* 564:71–76
62. Yissachar N, Salem H, Tennenbaum T, Motro B. 2006. Nek7 kinase is enriched at the centrosome, and is required for proper spindle assembly and mitotic progression. *FEBS Lett.* 580:6489–95
63. Guo C, Chi Z, Jiang D, Xu T, Yu W, et al. 2018. Cholesterol homeostatic regulator SCAP-SREBP2 integrates NLRP3 inflammasome activation and cholesterol biosynthetic signaling in macrophages. *Immunity* 49:842–56.e7
64. Misawa T, Takahama M, Kozaki T, Lee H, Zou J, et al. 2013. Microtubule-driven spatial arrangement of mitochondria promotes activation of the NLRP3 inflammasome. *Nat. Immunol.* 14:454–60
65. Subramanian N, Natarajan K, Clatworthy MR, Wang Z, Germain RN. 2013. The adaptor MAVS promotes NLRP3 mitochondrial localization and inflammasome activation. *Cell* 153:348–61
66. Liu Q, Zhang D, Hu D, Zhou X, Zhou Y. 2018. The role of mitochondria in NLRP3 inflammasome activation. *Mol. Immunol.* 103:115–24
67. Zhou R, Yazdi AS, Menu P, Tschopp J. 2011. A role for mitochondria in NLRP3 inflammasome activation. *Nature* 469:221–25
68. Paik S, Kim JK, Silwal P, Sasakawa C, Jo EK. 2021. An update on the regulatory mechanisms of NLRP3 inflammasome activation. *Cell Mol. Immunol.* 18:1141–60
69. Hayden FG, Herrington DT, Coats TL, Kim K, Cooper EC, et al. 2003. Efficacy and safety of oral pleconaril for treatment of colds due to picornaviruses in adults: results of 2 double-blind, randomized, placebo-controlled trials. *Clin. Infect. Dis.* 36:1523–32
70. Kim S, Lee K, Rhee K. 2007. NEK7 is a centrosomal kinase critical for microtubule nucleation. *Biochem. Biophys. Res. Commun.* 360:56–62
71. Fry AM, Bayliss R, Roig J. 2017. Mitotic regulation by NEK kinase networks. *Front. Cell Dev. Biol.* 5:102
72. Sun Z, Gong W, Zhang Y, Jia Z. 2020. Physiological and pathological roles of mammalian NEK7. *Front. Physiol.* 11:606996
73. O'Regan L, Fry AM. 2009. The Nek6 and Nek7 protein kinases are required for robust mitotic spindle formation and cytokinesis. *Mol. Cell. Biol.* 29:3975–90
74. Cohen S, Aizer A, Shav-Tal Y, Yanai A, Motro B. 2013. Nek7 kinase accelerates microtubule dynamic instability. *Biochim. Biophys. Acta* 1833:1104–13

75. Schmid-Burgk JL, Chauhan D, Schmidt T, Ebert TS, Reinhardt J, et al. 2016. A genome-wide CRISPR (clustered regularly interspaced short palindromic repeats) screen identifies NEK7 as an essential component of NLRP3 inflammasome activation. *J. Biol. Chem.* 291:103–9
76. Xu J, Lu L, Li L. 2016. NEK7: a novel promising therapy target for NLRP3-related inflammatory diseases. *Acta Biochim. Biophys. Sin.* 48:966–68
77. Byrne MJ, Nasir N, Basmadjian C, Bhatia C, Cunnison RF, et al. 2020. Nek7 conformational flexibility and inhibitor binding probed through protein engineering of the R-spine. *Biochem. J.* 477:1525–39
78. Richards MW, O'Regan L, Mas-Droux C, Blot JM, Cheung J, et al. 2009. An autoinhibitory tyrosine motif in the cell-cycle-regulated Nek7 kinase is released through binding of Nek9. *Mol. Cell* 36:560–70
79. Touitou I, Lesage S, McDermott M, Cuisset L, Hoffman H, et al. 2004. Infevers: an evolving mutation database for auto-inflammatory syndromes. *Hum. Mutat.* 24:194–98
80. Haq T, Richards MW, Burgess SG, Gallego P, Yeoh S, et al. 2015. Mechanistic basis of Nek7 activation through Nek9 binding and induced dimerization. *Nat. Commun.* 6:8771
81. Hochheiser IV, Behrmann H, Hagelueken G, Rodriguez-Alcazar JF, Kopp A, et al. 2022. Directionality of PYD filament growth determined by the transition of NLRP3 nucleation seeds to ASC elongation. *Sci. Adv.* 8:eabn7583
82. Masumoto J, Taniguchi S, Ayukawa K, Sarvotham H, Kishino T, et al. 1999. ASC, a novel 22-kDa protein, aggregates during apoptosis of human promyelocytic leukemia HL-60 cells. *J. Biol. Chem.* 274:33835–38
83. Moriya M, Taniguchi S, Wu P, Liepinsh E, Otting G, Sagara J. 2005. Role of charged and hydrophobic residues in the oligomerization of the PYRIN domain of ASC. *Biochemistry* 44:575–83
84. Masumoto J, Taniguchi S, Sagara J. 2001. Pyrin N-terminal homology domain- and caspase recruitment domain-dependent oligomerization of ASC. *Biochem. Biophys. Res. Commun.* 280:652–55
85. Lu A, Wu H. 2015. Structural mechanisms of inflammasome assembly. *FEBS J.* 282:435–44
86. Ferrao R, Wu H. 2012. Helical assembly in the death domain (DD) superfamily. *Curr. Opin. Struct. Biol.* 22:241–47
87. Oroz J, Barrera-Vilarmau S, Alfonso C, Rivas G, de Alba E. 2016. ASC pyrin domain self-associates and binds NLRP3 protein using equivalent binding interfaces. *J. Biol. Chem.* 291:19487–501
88. Gong Q, Robinson K, Xu C, Huynh PT, Chong KHC, et al. 2021. Structural basis for distinct inflammasome complex assembly by human NLRP1 and CARD8. *Nat. Commun.* 12:188
89. Xu Z, Zhou Y, Liu M, Ma H, Sun L, et al. 2021. Homotypic CARD-CARD interaction is critical for the activation of NLRP1 inflammasome. *Cell Death. Dis.* 12:57
90. Schmidt FI, Lu A, Chen JW, Ruan J, Tang C, et al. 2016. A single domain antibody fragment that recognizes the adaptor ASC defines the role of ASC domains in inflammasome assembly. *J. Exp. Med.* 213:771–90
91. Hollingsworth LR, David L, Li Y, Griswold AR, Ruan J, et al. 2021. Mechanism of filament formation in UPA-promoted CARD8 and NLRP1 inflammasomes. *Nat. Commun.* 12:189
92. Sanders MG, Parsons MJ, Howard AG, Liu J, Fassio SR, et al. 2015. Single-cell imaging of inflammatory caspase dimerization reveals differential recruitment to inflammasomes. *Cell Death. Dis.* 6:e1813
93. Evavold CL, Ruan J, Tan Y, Xia S, Wu H, Kagan JC. 2018. The pore-forming protein gasdermin D regulates interleukin-1 secretion from living macrophages. *Immunity* 48:35–44 e6
94. Heilig R, Dick MS, Sborgi L, Meunier E, Hiller S, Broz P. 2018. The Gasdermin-D pore acts as a conduit for IL-1β secretion in mice. *Eur. J. Immunol.* 48:584–92
95. Huang M, Zhang X, Toh GA, Gong Q, Wang J, et al. 2021. Structural and biochemical mechanisms of NLRP1 inhibition by DPP9. *Nature* 592:773–77
96. Shen C, Li R, Negro R, Cheng J, Vora SM, et al. 2021. Phase separation drives RNA virus-induced activation of the NLRP6 inflammasome. *Cell* 184:5759–74.e20